Latin American Journal of Solids and Structures
www.lajss.org

Severe Loading Assessment of Modern and New Proposed Beam to Column Connections

Abstract

The performance of two different steel beam to column connections known as SidePlateTM and a new proposed connection by seismic loading and progressive collapse were investigated in this research. Seismic performance evaluated included consideration of interstory drift angles and flexural strengths based on 2010 AISC Seismic Provisions while investigation of progressive collapse was conducted through satisfaction of acceptance criteria by rotational capacities of the connections provided in UFC 4-023-03 guideline. The results indicated that both SidePlate and the new proposed moment connection were capable of achieving adequate rotational capacity and developing full inelastic capacity of the connecting beam. Also, an excellent performance was exhibited by the connections in terms of keeping the plastic hinges away from the connection and exceeding interstory drift angle of 0.06 rad without fracture developments in beam flange groove-welded joints. Based on results, it was concluded that the SidePlate and the new proposed connection possess sufficient stiffness, strength and ductility to be classified as rigid, full-strength and ductile connections.

Keywords
SidePlateTM moment connection, interstory drift angle, progressive collapse, seismic performance.

Iman Faridmehr [a*]
Mohd Hanim Osman [a]
Mamood Md. Tahir [a]
Ali Farokhi Nejad [b]
Reza Hodjati [c]

[a] UTM Construction Research Centre (CRC), Faculty of Civil Engineering, Universiti Teknologi Malaysia (UTM), Skudai, Johor Bahru, 81300, Malaysia.
[b] Faculty of Mechanical Engineering, Universiti Teknologi Malaysia (UTM), Skudai, Johor Bahru, 81300, Malaysia
[c] Department of Civil Engineering, Shahrood Branch, Islamic Azad University, Shahrood, Iran
* Corresponding author: Iman Faridmehr
s.k.k-co@live.com

http://dx.doi.org/10.1590/1679-78251286

Received 15.04.2014
In Revised Form 26.10.2014
Accepted 05.01.2015
Available Online 07.02.2015

1 INTRODUCTION

Technological advance of many proprietary connections commenced after the 1994 Northridge earthquake as a result of development of brittle fractures at some steel moment resisting connections such as welded beam-flange-to-column-flange joints. This unanticipated brittle fracture was against the projected design philosophy and behavior of these frames, which was energy dissipation

through formation of ductile plastic hinges in steel beams. At present, quality acceptance of all moment resisting connections incorporated in special or intermediate steel moment frames is undertaken through conduction of tests applying the protocol designated in Appendix S of the AISC Seismic ProvisionsConstruction (2010) . This specific connection test endeavors to highlight the ability of the connection in withstanding large inelastic deformations through controlled ductile yielding in specific behavioral modes. Apropos of the seismic performance of steel moment frames, several research programs have been carried out by the Federal Emergency Management Agency "FEMA" Agency (2000) in the US and in addition, various reports on seismic design of steel beam column connections, such as FEMA 350 Agency (2000)and FEMA 351 Agency (2000), have been published to provide the required information for seismic design purposes. For instance, verification of the seismic performance of the Post-Northridge (PN) connections was implemented using both the FE modeling and full-size experiments Jones *et al.* (2002, Kim *et al.* (2002, Ricles *et al.* (2002, Hedayat and Celikag (2009, Saffari *et al.* (2013, Beland *et al.* (2014, Han *et al.* (2014, Sofias *et al.* (2014).

Several cases of partial or total progressive collapse under extreme abnormal loading conditions resulting from fires, impacts, or explosions have been experienced by buildings throughout the world over the past few decades. Despite the rare possibility of building collapse incidents, the consequent casualties and property loss could not be ignored. Therefore, the increasing trend of designing progressive collapse resistant buildings has been expedited after the 9/11 terrorist attacks in 2001 which resulted in the total collapse of the World Trade Center buildings Sabuwala *et al.* (2005) Jalali *et al.* (2012) Chou *et al.* (2010) Kim *et al.* (2011) Khandelwal and El-Tawil (2011) Liu (2010) Yang and Tan (2013) Sun *et al.* (2012) Olmati *et al.* (2013). A practical guideline was introduced by The U.S. General Services Administration (2003) to reduce the collapse potential of federal buildings along with a guideline for the new and existing DoD buildings presented by the UFC 4-023-03 Department of Defense (2010). The Alternative Path (AP) method is the analysis procedure proposed by these guidelines. In this design approach, failure of one component will not result in general collapse of the structure and this resistance is attributed to the presence of alternate paths within the structure. In most design-for-redundancy cases, tolerating the loss of any one column without collapse would be the uttermost requirement. Once a column is removed from the structure, the vertical loads of the structure will be resisted by the flexural capacity of the beams on both sides of the removed column. Since the beams have to tolerate significant inelastic rotations and large deflections, their behavior will resemble cables. At fairly large deflections, the main resistance to the applied loads will be provided by the catenary action of the beams Khandelwal *et al.* (2009). Hence, a thorough progressive collapse resistant analysis and design enforces a comprehensive understanding of the interaction of moment and axial tension in the beams including their connections during the entire progression of load transfer. Yet, this issue is still under investigation and no rational methodologies have been propounded to explicitly comprehend the moment and axial tension interaction for practical design applications.

This study is comprised of numerical and experimental investigations regarding progressive collapse and earthquake-resistant capacities of the SidePlate and a new proposed moment connection system. The models were scaled down to 1/6 of their real size and were finally set up in the Laboratory of Structures and Materials, Universiti Teknologi Malaysia (UTM), so that they could be com-

pared with the material and geometric nonlinear FEA results obtained from the general purpose FEA software ABAQUS. Interstory drift angles and flexural strengths recommended by AISC Seismic Provisions were considered for seismic assessment while the rotational capacities of the connections based on the acceptance criteria provided by UFC 4-023-03 guideline were supposed to be satisfied to resist the progressive collapse phenomenon.

2 RESEARCH METHODOLOGY AND MODELING SETUP

2.1 Case Studies and Design Procedures

Steel Special Moment Frame (SMF) and Intermediate Moment Frame (IMF) systems are composed of beam-to-column moment connections prefabricated by SidePlate connection technology. The beam ends in this type of connection are not directly linked to the columns; instead, two strong full-depth SidePlates are incorporated to sandwich beam ends to the columns and therefore, the expected stress concentration at the beam-to-column interface, common in ordinary welded detailing vulnerable to brittle weld fracture, will be eliminated. In addition, termination of excessive shear distortion of the panel zone will occur in this type of connection and this is due to presence of two thick SidePlates acting in conjunction with column webs. Hence, both the stress concentration resulting from this high stiffness and the fracture in weld metal will be eliminated eventually. It is noteworthy to mention that all applicable requirements of the 2009 IBC (2006) and 2010 AISC Seismic Provisions are satisfied by SidePlate moment connection systems. In the test program, mathematically scaled models reduced to 1/6th of the real size of the section properties in SidePlate connection system were manufactured in the laboratory in conformance with the provisions of SidePlate Systems, Inc. and were employed in the design/analysis of the beams and columns as well as the fully rigid panel zone modeling.

In the proposed moment connection system, the beam ends are not directly attached to the column and instead, they are sandwiched to the flanges of the column. Therefore, to successfully distribute all the gravity and lateral loads in addition to bending moments of the two beams used in this connection, plates were groove welded to the top and bottom flanges of both beams and positioned vertical to the axis of the beams. Furthermore, calculation of the section properties for the proposed connection was conducted in conformance with the requirements of 2010 AISC Seismic Provisions and Prequalified Connections for Special and Intermediate Steel Moment Frames for Seismic Applications "ANSI/AISC 358-10" Construction (2010) guideline. Figure 1 highlights the case studies incorporated in this research. Since seismic and progressive collapse assessment of three different steel moment connections are the main objectives of this study, an attempt has been made to use columns with same section properties in all three connections. Also, an equal moment of inertia was recorded for both the two beams of new proposed connection and the beams of SidePlate while considering all the seismic provisions of the compact sections (Table 1).

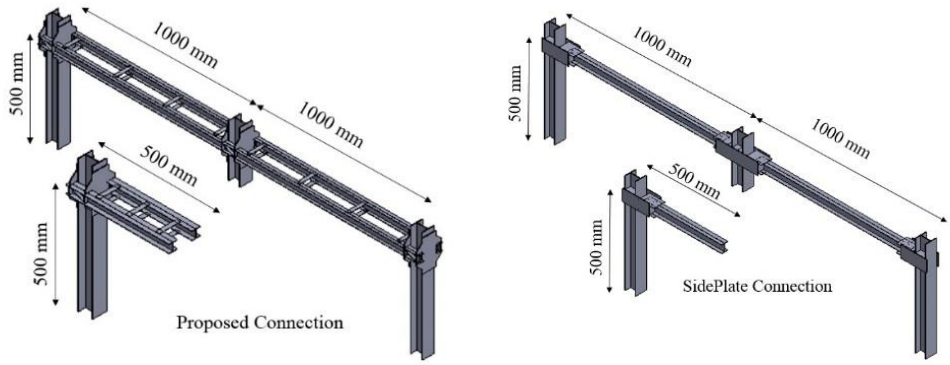

Figure 1: Case Studies for Seismic and Progressive Collapse Assessment.

Element	Size (mm)	Cross-section	Moment of Inertia (mm4)
Beam section (SidePlate)		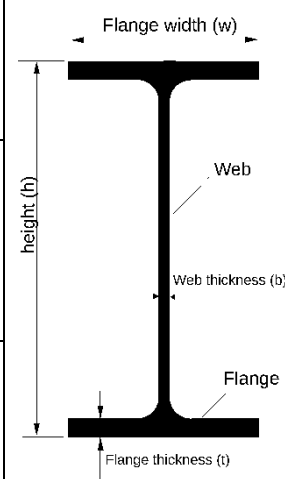	1040×10^2
height			
Web thickness	50		
Flange width	2		
Flange thickness	40		
	2		
Beam section (Proposed Connection)*			492×10^2
Height	40		
Web thickness	1.5		
Flange width	30		
Flange thickness	2		
Column section			6900×10^2
Height	70		
Web thickness	4		
Flange width	70		
Flange thickness	4		

* Notice that the proposed connection possesses two beams.

Table 1: Beam, column and connection sections selected in this study.

2.2 Fabrication and Modeling Setup

Fabrication of the test specimens was performed by collaboration of both the university laboratory personnel and commercial fabricators. Gas Metal Arc Welding (GMAW) was the type of welding used in this project. GMAW – commonly referred to as Metal Inert Gas (MIG) – welding includes a group of arc welding processes in which powered feed rolls (wire feeder) feed a continuous electrode (the wire)) into the weld pool (Figure 2). An electric arc is made between the weld pool and the tip

of the wire. Melting of the wire is implemented progressively at the same speed at which it is being fed and thus, part of the weld pool is formed. To effectually protect both the arc and the weld pool from atmospheric contamination, a shield of inert (non-reactive) gas will be delivered through a nozzle concentric with the welding wire guide tube. This welding application is beneficial in terms of speed, continuity, comparative freedom from distortion and the reliability of automatic welding in addition to control and versatility of manual welding. There has been an escalating trend of using this technique in mechanized set-ups. In this project, a handheld gun was hired to carry out MIG welding as a semiautomatic process. Generally, welding parameters are comprised of travel speed, voltage, arc (stick-out) length and wire feed rate set to plate thickness. Hence, the filler metal transfer method was adopted considering the arc voltage and wire feed rate. Once the welding process was finished, the specimens were coated with lime for the purpose of facilitation of yielding observation within the connection region.

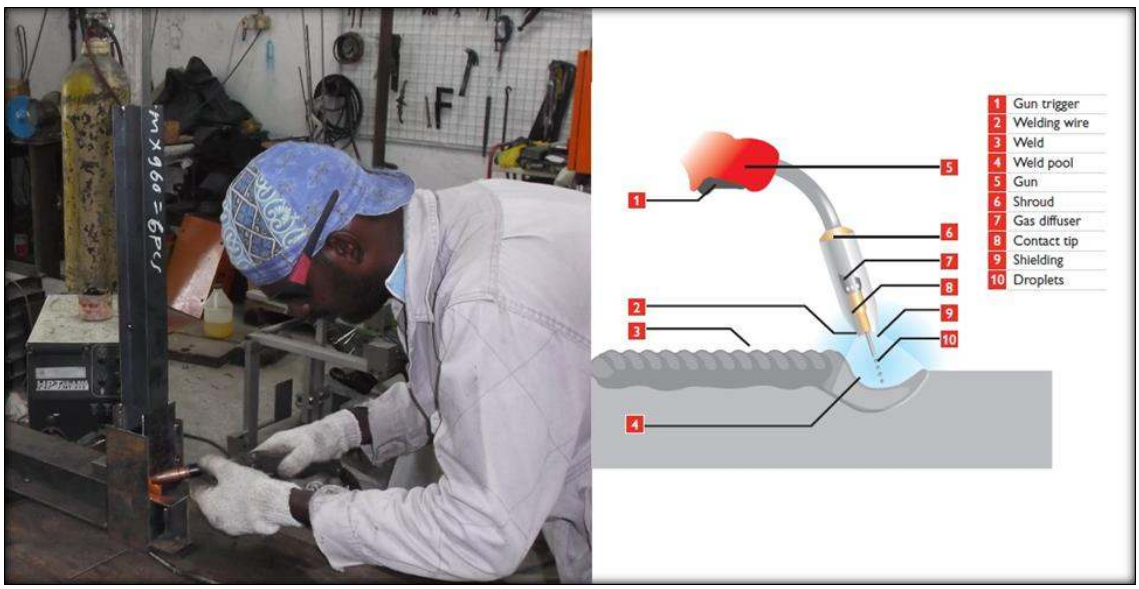

Figure 2: Schematic View of Welding Transfer and Accessories.

Different loading protocols and lateral restraint assemblies were considered for the 1/6th scale testing set-ups regarding the progressive collapse and seismic assessment of the specimens (Figure 3). The missing column scenario (AP method) was applied for the progressive collapse test where the interior column was selected as the missing column assumed to have been instantaneously destroyed by a devastating event. A monotonically increasing "ramp" was used to simulate the quasi static loading adopted for this project (Figure 4). A hydraulic actuator to the tip of the beam was incorporated to conduct and evaluate the cyclic test of the seismic specimens. A 250-kN-capacity for compression and a 250-kN-capacity for tension and a maximum piston stroke of 500 are the specifications of the Hydraulic pseudo-dynamic actuator used in this research (Figure 4). Both sides of the beams were laterally restrained at locations 150 and 800 mm from the centerline of the specimen column. Likewise, both sides of the beams were laterally restrained at middling length of beam from the centerline of the specimen column. Finally, evaluation of the seismic behavior was performed

through conduction of a cyclic test by a hydraulic actuator to the tip of the beam. Other assumptions used for this experiment are as follows:

I. The tests were two-dimensional only and specimens were constrained in plane. The impact of out-of-plane beams concurring to the joint was neglected.

II. Slab effects were neglected ("conservative" approach).

III. The assumed initial conditions of the specimens were zero stress resulting from gravity and live loads and zero velocity.

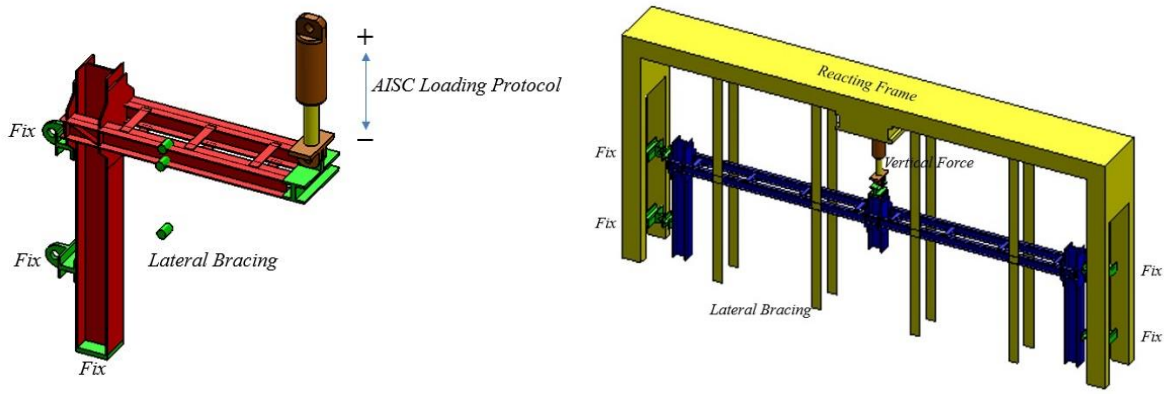

(a) (b)

Figure 3: Modeling Set Up For Seismic (a) and Progressive Collapse Assessment (b).



(a) (b)

Figure 4: The Dynamic Actuator (a) and Hydraulic Jack (b) Used For Seismic and Progressive Collapse Evaluation.

The fundamental scaling factors used to convert a scaled-down model to a full-scale one are the scaling factor for length, S1, the scaling factor for the material elastic modulus, SE, the scaling factor for strain, Sε, the scaling factor for stress, Sσ and the scaling factor for mass, SM (mass scaling

is particularly used in dynamic simulations). Since both the prototype and model are both made of the same steel material, S_E=1. The following equations are used to calculate the previous mentioned scaling factors which summarized in Table 2:

$$S_l = \frac{\text{Prototype length}}{\text{Model length}} = \frac{6}{1} = 6 \tag{1}$$

$$S_\varepsilon = \frac{S_{\Delta L}}{S_L} = 1 \tag{2}$$

$$S_\sigma = S_E\, S_\varepsilon = 1 \tag{3}$$

Quantities	Symbol	Scale Factor Value
Material-Related Properties		
Modulus of Elasticity	S_E	1
Strain	S_ε	1
Stress	S_σ	1
Poisson's Ratio	υ	1

Table 2: Scale factor values calculated for this study

2.3 Finite Element Modeling Procedure

The FE software ABAQUS/STANDARD was incorporated to perform the numerical phase of the study. For the purpose of getting a better response from the structure, the solid C3D8R element having eight nodes with six degrees of freedom has been used which represents three force components and three moment components simultaneously. The true stress-strain curve has been used to model the material behavior. The following formulas for displacements and strains are introduced for the purpose of FE representation:

$$e = \frac{\Delta l}{l} \tag{4}$$

$$S = \frac{P}{A_0} \tag{5}$$

$$\sigma = s(1+e) \tag{6}$$

$$\varepsilon = ln(1+e) \tag{7}$$

Where; e and S are engineering strain and stress respectively calculated from uniaxial tensile test and consequently, σ and ε are the true stress and strain determined from the above equations. The true and engineering stress-strain curves along with the universal testing machine used to conduct the tests are presented in Figure 5.

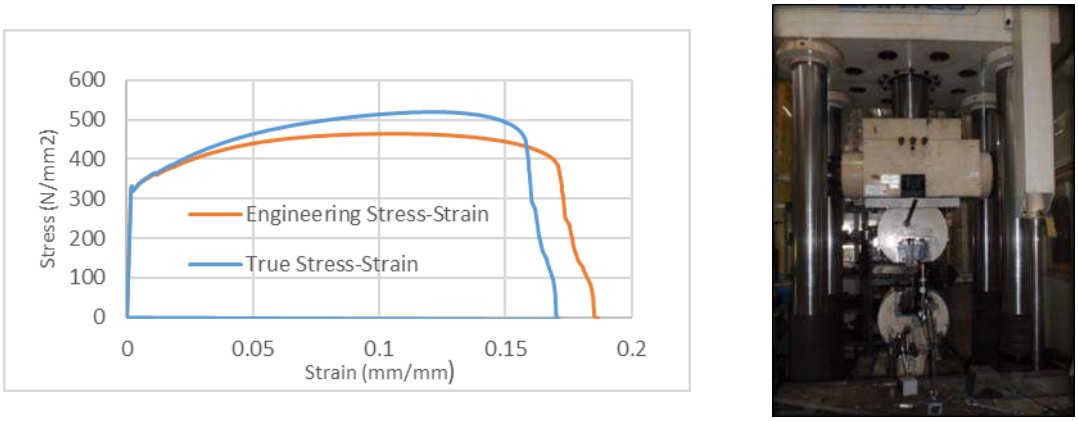

(a) (b)

Figure 5: Material Properties for True Stress-Strain and Engineering Stress-Strain (a) and Universal Testing Machine (b).

After the conduction of tensile testing, the yield stress and ultimate tensile strength were 320MPa and 510MPa respectively. In the FE model, load application through displacement control in vertical direction along with fixing the column base in all degrees of freedom was carried out in all cases. A loading rate of 2mm/s assuming to be quasi static was selected. Also, the hex element was incorporated in all models to achieve a finer-size mesh in the connection area.

2.4 Loading Protocol

The 2010 AISC Seismic Provisions were considered in seismic evaluation of the loading sequence used in this study. A series of load steps and the required number of cycles for each one are specified in AISC Protocol (Figure 6). Each total interstory drift angle is corresponded to a load step. The testing began with application of load steps along with recording the data points at regular intervals. Then, at the end of each load step, photographs were taken and observations were recorded as well. Once the strength of the specimen decreased to 40 percent of the maximum strength, the loading was stopped. For the purpose of progressive collapse assessment, the vertical push-down analysis through gradually increasing the vertical displacement at the loc`ation of the removed column was conducted to determine the connection rotational capacity and resistance of the structure against such deformation.

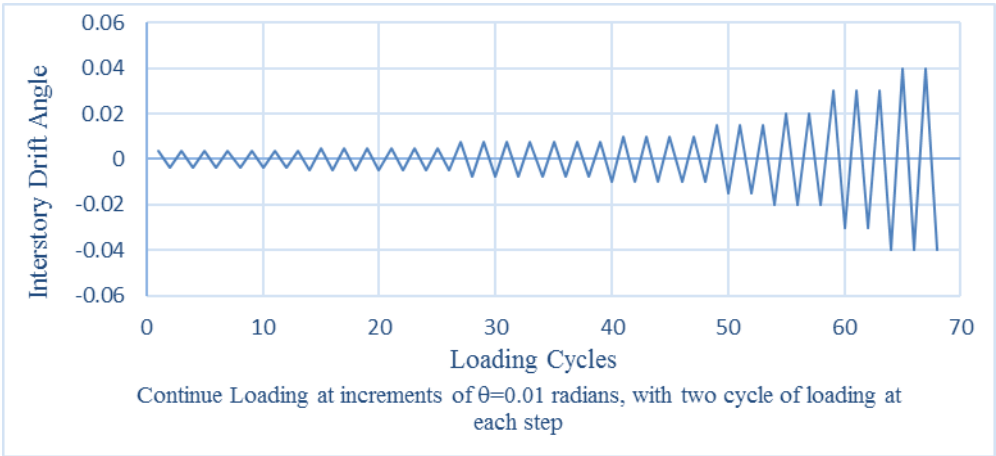

Figure 6: The Loading Protocol Used For Seismic Assessment.

2.5 Acceptance Criteria Based on 2010AISC Seismic Provisions and UFC 4-023-03

According to 2010 AISC Seismic Provisions , provision of substantial inelastic drift capacity through flexural yielding of the SMF beams and limited yielding of column panel zones must be considered in the design of the SMF. Moreover, the design of the columns shall be stronger than those of fully yielded and strain-hardened beams or girders. In the end, the following requirements must be satisfied for beam-to-column connections applied for seismic evaluation:

I. An inter story drift angle of at least 0.04 rad must be sustained by the connection (Figure 7a).

II. The flexural resistance of the connection measured at the column face shall be equal to at least 0.80Mp of the connected beam at an inter story drift angle of 0.04 rad.

The fundamental principal in arresting progressive collapse would be adequate connection rotational capacity (Figure 7b). Although moment connections are prequalified for rotational capacity resulting from bending alone, they fail to resist the interaction of axial tension and bending moment, essential to prevent progressive collapse, simultaneously. While the load carrying capacity of the system over bending moment alone could significantly be increased by tension stiffness ('cable-like' action), the large flange tension forces developed from the combination of bending moment and axial tension must be transferred by the beam-to-column connection. Table 5-2 of UFC 4-023-03 demonstrates the design strength and rotational capacities of the beam-to-column connections incorporated in progressive collapse assessment (Table 3).

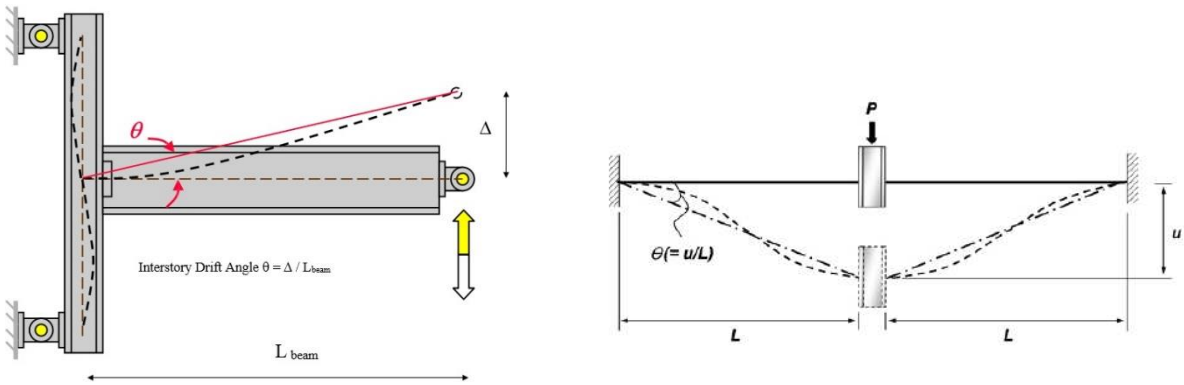

(a) (b)

Figure 7: Definition of Interstory Drift Angle (a) and Connection Rotation Capacity (b).

Connection type	Plastic rotation angle (θ), radians	
SidePlate™	primary	secondary
	0.089-0.0005d	0.169-0.0001d
d = depth of beam, inch		

Table 3: Acceptance Criteria for Fully Restrained Moment Connections.

3 RESULTS AND DISCUSSION

3.1 Progressive Collapse Assessment

The typical behavior of the double-span beams based on FEA and experimental results are discussed in this section. The key variable in assessment of progressive collapse phenomenon would be the plastic rotation angle (θ) defined as the vertical deflection of the column (u) divided by the clear span length of the beam (L) (Figure 7).

3.1.1 SidePlate Connection Specimen

Based on the data collected by direct observation, photographic documentation and data logger, it was concluded that at first stage of failure, formation of plastic hinges occurred at the quarter beam depth from the end of the SidePlate at a vertical load of 6.5 kN. At this stage, a slight but visible buckling occurred in beam flanges. The strain gauge readings, which were above the yielding level of 1800 με (micro-strain), verified the formation of plastic hinges. At later stages of the push-down, the quarter beam depth from the end of the SidePlate experienced full formation of the expected

plastic mechanism. Yet, the outstanding fact regarding the SidePlate was observation of significant global hardening. This issue is an indication of the fact that the SidePlate is capable of developing the full capacity of connected beams. It is noteworthy to mention that during the vertical loading process of 10 to 15 kN, the majority of the strain gauges were well beyond yield level and demonstrated recorded strains of 5000 με (i.e. almost 3 times above the yield level). At the vertical load of 19 kN and plastic hinge rotation angle of around o.2 rad, a series of fractures appeared at beam flanges. At this stage, degradation and demise of the SidePlate specimen began due to progressive collapse phenomenon. The obvious fact was the good performance of the SidePlate moment connection in developing the catenary action once it reached to large vertical displacements. The main failure modes of the SidePlate are marked as follows: (i) plastic rotation of members (plastic hinges), (ii) inelastic local buckling of web or flange of steel sections for beams (which in some extreme cases results in fractures), (iii) initiation of fracture within the flange at the tension side of the beam with consequent propagation to the web. Figure 8 is an illustration of the damaged state of the specimen and plastic equivalent strain distribution after the final stage of progressive collapse test.

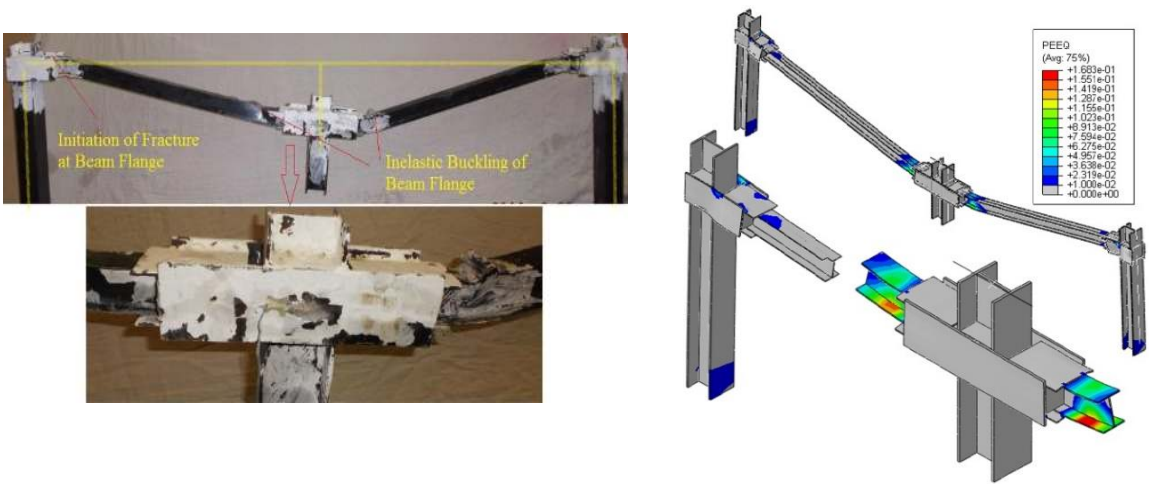

(a) (b)

Figure 8: Damaged State at the End of Progressive Collapse Test (a) and Plastic Equivalent Strain Distribution (B).

The numerical and experimental visualized plots of vertical load versus the plastic hinge rotation angle of the progressive collapse tests for the SidePlate specimen is illustrated in Figure 9. Based on the presented data, the experimental and numerical results of the tests regarding the yield point, strain hardening, modes of failure and maximum plastic hinge rotations are in good agreement.

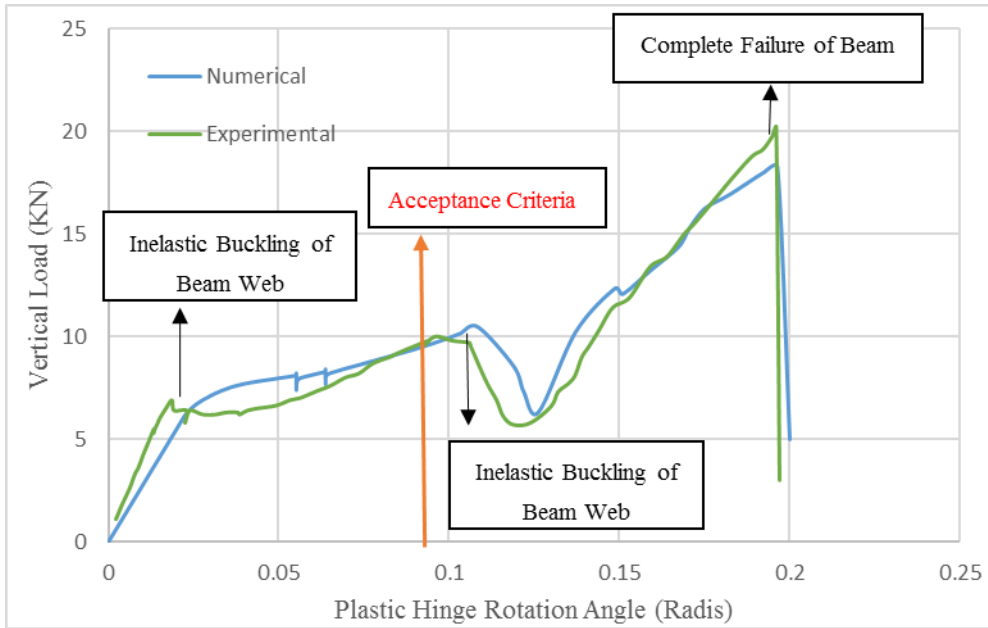

Figure 9: Force vs. Plastic Hinge Rotation Angle for Progressive Collapse Tests.

3.1.2 New Proposed Moment Connection Specimen

According to the data collected by direct observation, photographic documentation and data logger, it was concluded that at first stage of failure, formation of plastic hinges occurred at the beam top flange between two connection plates at vertical load of 6.7 kN. Also, rotation concentration along with increasing deflections at the mid-span was observed at this location. Furthermore, experienced significant global hardening and plastic hinge formations were occurred at the beams only similar to that of the SidePlate connection. Failure of the proposed moment connection occurred at a vertical load of around 18.6 kN and plastic hinge rotation angle of around o.22 rad, which was determined by dividing the center-column displacement at failure by the center line to- center line beam span. Considering the nominal yield strain of 1800 με (micro-strain), higher strain readings in the range of 5000 to 5800 με (i.e. almost 3 times above the yield level) were obtained at beam flanges indicating that the beams were in the plastic range during the testing process. These strain readings showed the severe axial forces experienced by the beams to develop catenary action. On the other hand, the beam continuity plates and column flanges delimited the strains at the column shear zone and the column web portion and therefore, the connection plate maintained its elastic behavior throughout the loading scenario. The main failure modes of the proposed moment connection are marked as follows: (i): inelastic local buckling of the top beam flanges and webs and (ii): fracture initiation at at the flange at the tension side of the beam along with consequent propagation to the web. Figure 10 indicates the damaged state of the proposed moment connection specimen along with the plastic equivalent strain distribution after the final step of progressive collapse test.

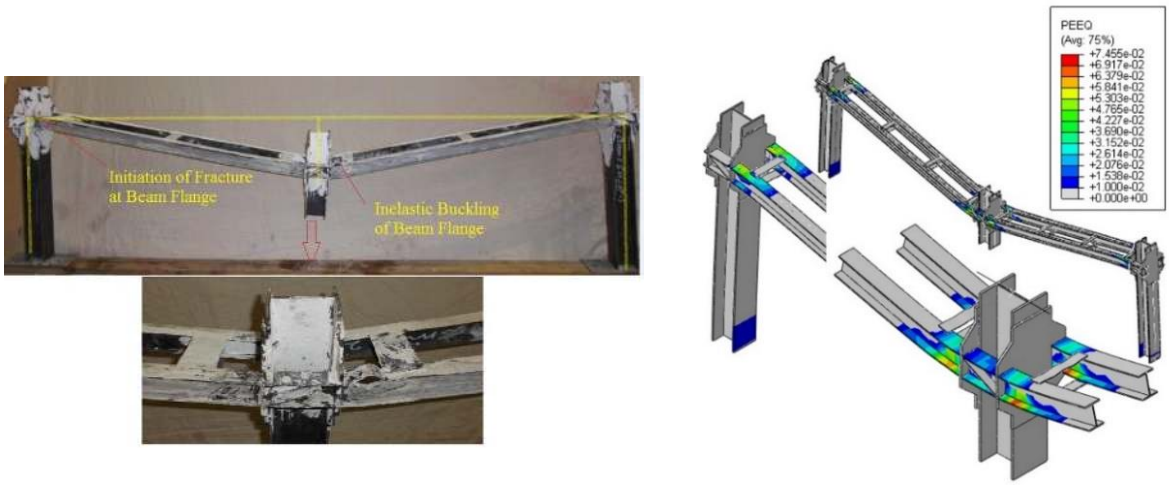

(a) (b)

Figure 10: Damaged State at the End of Progressive Collapse Test (a) and Plastic Equivalent Strain Distribution (b).

The numerical and experimental visualized plots of vertical load versus the plastic hinge rotation angle of the progressive collapse tests for the proposed moment connection specimen is illustrated in Figure 11. Similar to the SidePlate specimen, the experimental and numerical results of the tests regarding the yield point, strain hardening, modes of failure and maximum plastic hinge rotations are in good agreement. Notice, the acceptance criteria for the proposed new connection have been chosen similar to that of the SidePlate connection.

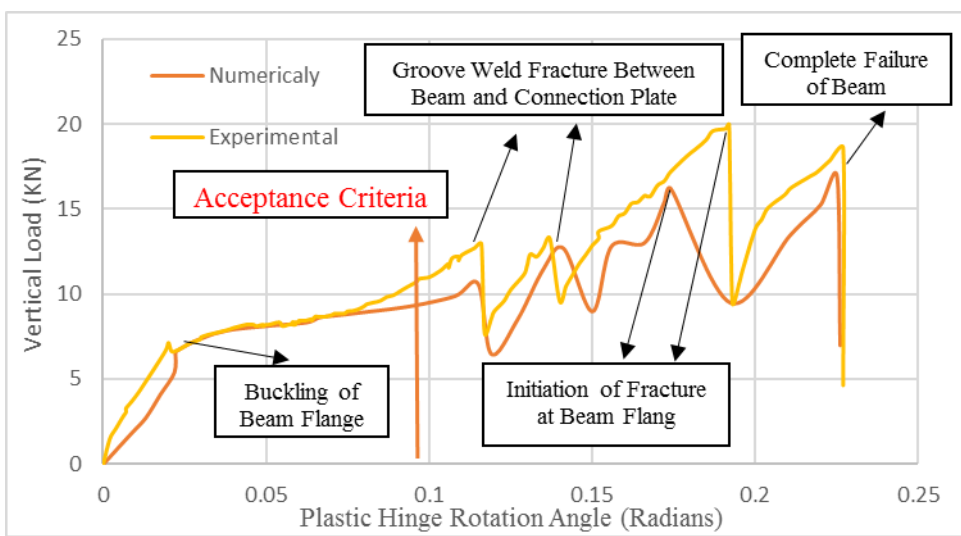

Figure 11: Force vs. Plastic Hinge Rotation Angle for Progressive Collapse Tests.

A comparison between the recorded experimental (test) and numerical (analysis) results of the progressive collapse performance of the connection types tested in this project is presented in Table 4.

Moment connection type	Vertical Force at First Fracture (KN)		Max Vertical Force at End of Test (KN)		Joint Rotation at First Fracture (Radians)		Joint Rotation at End of the Test (Radians)		Mode of Failure	
	Analysis	Test	Analysis	Test	Analysis	Test	Analysis	Test	Analysis	Test
SidePlate	10.4	10	18.2	20.2	0.1	0.1	0.19	0.19	Beam Failure	Beam Failure
New Proposed Connection	10.6	12.9	16.9	18.6	0.11	0.11	0.22	0.22	Beam Failure	Beam Failure

Table 4: Result summaries of progressive collapse evaluation.

3.2 Seismic Assessment

The seismic performance of all the three different connections will be discussed in this section. Interstory drift angle is known to be the fundamental parameter in investigation of the seismic performance of structures as illustrated in Figure 7.

3.2.1 SidePlate Connection Specimen

Once minor flaking of the whitewash coating of top beam flange region was observed during the first cycle of 0.015 story drift cycles, the first yielding of the SidePlate Connection Specimen occurred. The yielding became more noticeable after 0.02 story drift cycles. Although no signs of yielding were detected in the SidePlates and the beam cover plates during the 0.03 story drift, the entire beam flange showed signs of yielding. Yet, the peak strength was reported for this interstory drift angle. The groove weld between the shear plate and column face experienced a minor fracture at an interstory drift angle of 0.04 rad. A slight decrease in strength was observed towards the interstory drift angle of -0.04 rad resulting from the inelastic buckling of the beam top flange. This top flange buckling was followed by the beam web buckling despite its very small amplitudes. Then, the groove welding between beam top flange and beam web showed some cracks at an interstory drift angle of 0.05. Next, formation of low cycle fatigue cracks was observed in the base metal at beam top flange. After that, during the first cycle of 0.06 story drift, more extensive cracks appeared on as they extended down into the web plate. Although no column or panel zone yielding took place during the test, one complete cycle of an interstory drift angle of 0.06 was resisted by the SidePlate connection specimen. Finally, once fractures in the web and in the top flange of the beam were noticed, the test stopped. At final stage of the test, the strain gauges positioned on beam

flanges demonstrated records beyond 4800 με (micro-strain) which was an indication of development of fully plastic capacity of connecting beams. The experimental failure mode and the plastic equivalent strain distribution at the end of cyclic test are demonstrated in Figure 12.

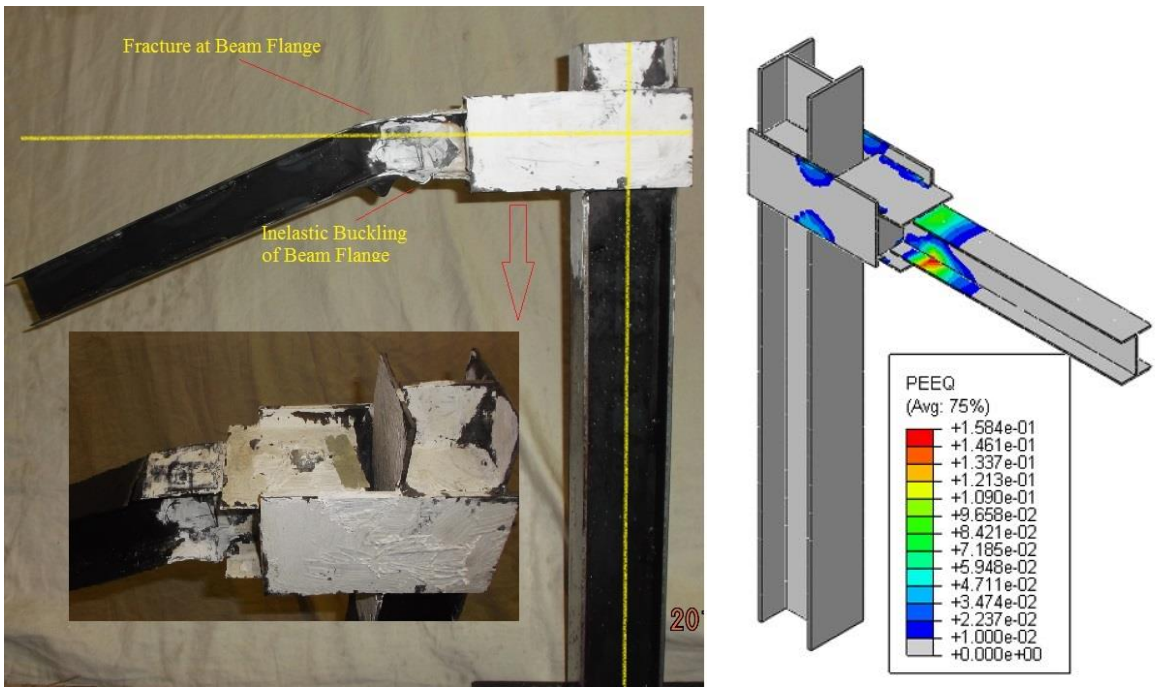

Figure 12: Damaged State at the End of Seismic Test & Plastic Equivalent Strain Distribution.

The global seismic response of the connection is illustrated in Figure 13, which is the computed moment at the column face versus interstory drift angle. The results of the numericl model and the experimental test were in good agreement in the overall cyclic behavior. Also, formation of plastic hinges at the beam flange was confirmed by the numerical results. No signs of degradation were detected in the hysteretic responses of the Specimen during the FEA. Nevertheless, initiation of local buckling of the beam flange at an interstory drift angle of 0.05 resulted in a decrease in the hardening slope along with a flattening of the curve during the last cycles. All in all, yielding and buckling patterns of the numerical model and experimental test results were in good agreement.

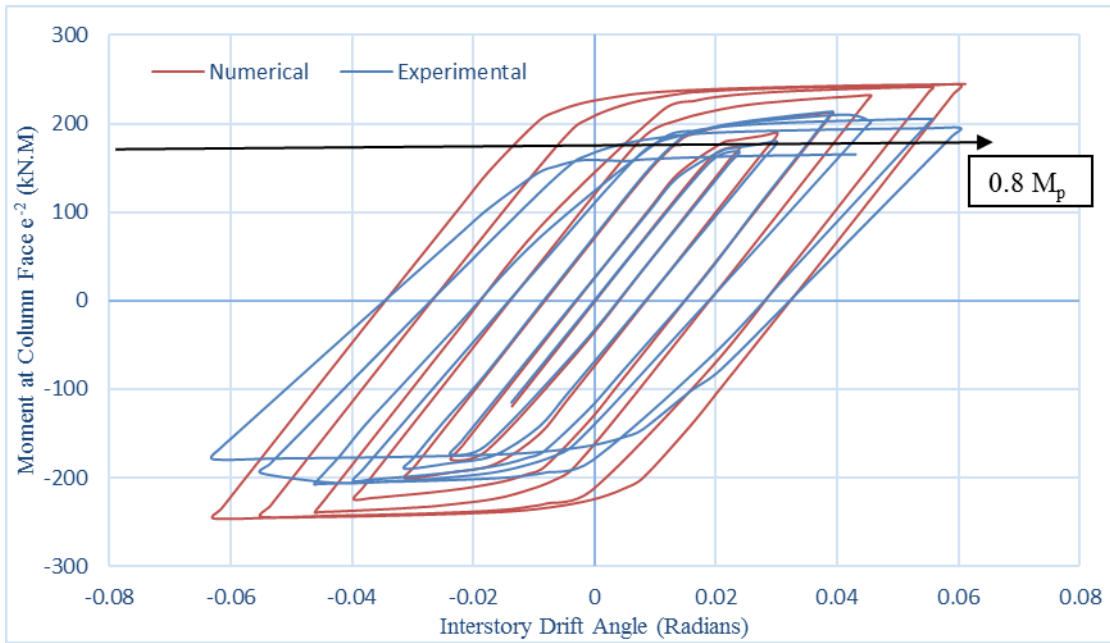

Figure 13: Moment at column face versus interstory drift angle.

3.2.2 New Proposed Moment Connection Specimen

An excellent performance was observed for the proposed moment connection specimen under cyclic loading. Similar to SidePlate connection specimen, only the beam formed a real plastic hinge. Also, the ductility which is referred to as the interstory drift angle was higher than 0.06 rad. Signs of initial yielding were observed during the first cycle at 0.02 radians at the bottom flange. Yielding propagation along the beam flange between two connection plates started by progressing through the loading history. The connection plate also showed signs of yielding during the first cycle of 0.03 radians. In addition, signs of web buckling adjacent to the yielded bottom flange were observed during the second cycle of 0.03 radians. Next, at the cycle of 0.04 radians, local buckling of the bottom flange was developed. The fact that the column panel zone remained in elastic area during these cycles is of great importance. After each successive loading cycle, the local buckling of flange became more evident. The outstanding issue regarding the bottom flange and web buckling was lack of significant deterioration in the hysteresis loop. Since groove welding fracture initiated between flange and connection plate along with as inelastic buckling at beam flange, slight strength degradation was observed after the cycle of 0.05 radians. Although no column or panel zone yielding was detected during the test, the proposed moment connection was capable of resisting one complete cycle of interstory drift angle of 0.06 rad. In conclusion, formation of extensive plastic hinges at the beam flanges region plus measured strain values of 4500 με (micro-strain) recorded by the strain gages installed at beam flanges confirmed the excellent performance of the proposed moment connection under cyclic loading. The experimental failure mode and the equivalent strain distribution at the end of cyclic test are demonstrated in Figure 14.

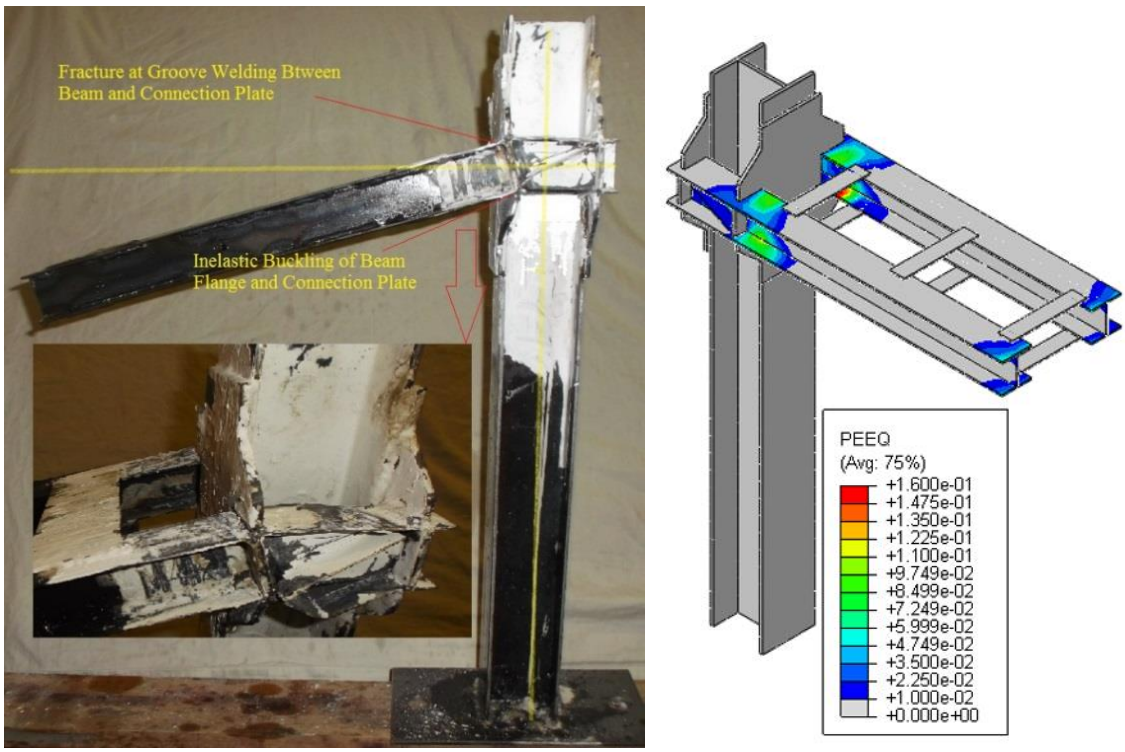

Figure 14: Damaged State at the End of Seismic Test & Plastic Equivalent Strain Distribution.

Figure 15 highlights a reasonable correlation between the numerical and experimental results of the proposed moment connection, particularly in the elastic region where negligible divergences are present. The plastic strain distribution at 0.06 story drift confirms the complete formation of plastic hinges in the same location with experimental test and therefore, concentration of plastic deformations therein. Based on the numerical results, very low levels of plastic strains were experienced by the connection plates and the panel zones and development of inelastic deformation mostly occur in the beam's plastic hinge. The maximum Von Mises strain, developed in the proposed connection model at the beam flange, was about two times bigger than strain in the beam web. In general there is a good agreement between the experimental and numerical results.

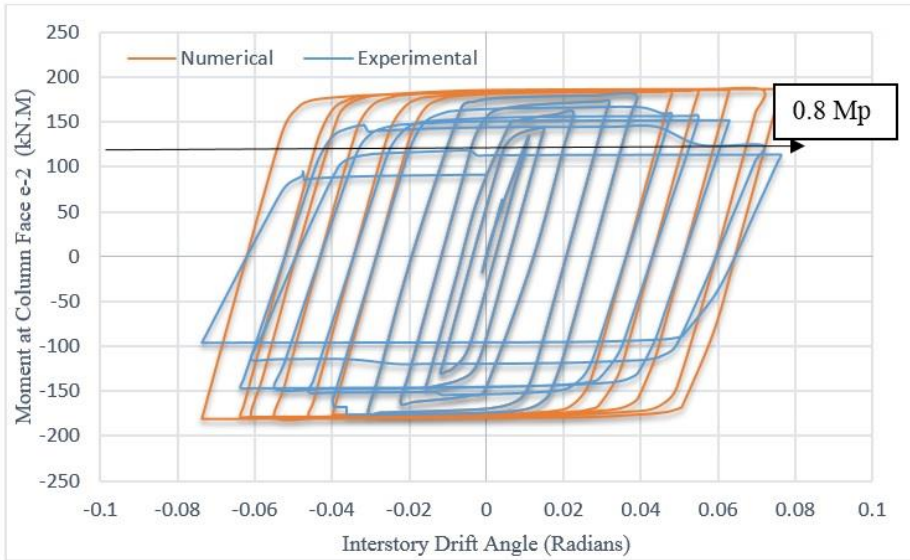

Figure 15: Moment at column face versus interstory drift angle.

A comparison between the recorded experimental (test) and numerical (analysis) results of seismic evaluation for the three different connection types namely the SidePlateTM and proposed moment connection is presented in Table 5.

Moment connection type	M/M_p First Fracture		M/M_p Maximum		Interstory Drift Angle at First Fracture (Radians)		Interstory Drift Angle at Failure Point (Radians)		Mode of Failure	
	Analysis	Test	Analysis	Test	Analysis	Test	Analysis	Test	Analysis	Test
SidePlate	1.20	1.08	1.28	1.25	0.05	0.04	0.07	0.06	Beam Failure	Beam Failure
New Proposed Connection	1.10	1.18	1.35	1.28	0.04	0.05	0.06	0.06	Beam Failure	Beam Failure

Table 5: Results summaries of seismic evaluation.

4 STIFFNESS DEGRADATION AND ENERGY DISSIPATION CAPACITY

An investigation on the stiffness retention capacity of the test specimens was conducted through the analysis of the lateral peak-to-peak stiffness measured during the each level of story drift. Calculation of the lateral stiffness, k, was performed at each cycle through dividing the peak lateral force applied at each cycle over the displacement measured in the subassembly at that specific cycle (Figure 16). The lateral stiffness values measured during the tests for the two specimens are demonstrated in Table 6. In this table, it is observed that a similar response characterized by an almost linear decay in lateral stiffness was observed for the two specimens. Yet, the new proposed connection turned out to be the stiffest specimen during the cycles performed at story drift values larger than 4.0%. This stiffer behavior is attributed to the distribution of hinge formation mechanism due to the presence of two beams in the connection which result in increased stiffness of the subassembly. Besides, the SidePlate specimen indicated very similar stiffness values for lateral deformations prior to 4.0% drift compared to those of the new proposed connection as a result of the two side plates wrapping around the shear panel joint region.

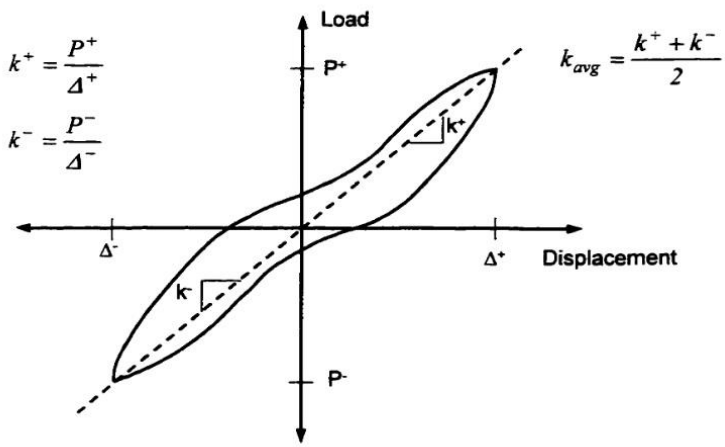

Figure16: Definition of the lateral peak-to-peak stiffness.

Specimen	Interstory Drift Angle (Radians)						
	1 %	2%	3%	4%	5%	6%	7%
Sideplate	0.18	0.205	0.215	0.25	0.17	0.1	.055
New Proposed	0.123	0.18	0.21	0.225	0.215	0.14	0.095

Table 6: Lateral peak-to-peak stiffness (KN/mm).

The total energy dissipated and the equivalent viscous damping ratio of the subassemblies was hired to study the energy dissipation capacity of the test specimens. Determination of the total energy dissipated by specimens was done through an area enclosed by the load vs. displacement hysteresis loop for each cycle (Figure 17). The magnitude of energy dissipated by each specimen is a

function of the applied lateral load along with the shape of the load vs. displacement hysteresis loops. The total amount of energy dissipated throughout the cyclic test at each level of story drift for the two specimens is illustrated in Figure 18. According to Figure 18, adequate energy dissipation capacities with no signs of degradation were observed for both the SidePlate and new proposed connection until 0.06 interstory drift angle.

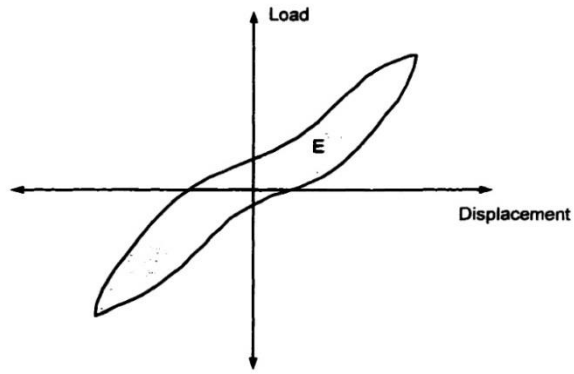

Figure 17: Energy dissipated per cycle.

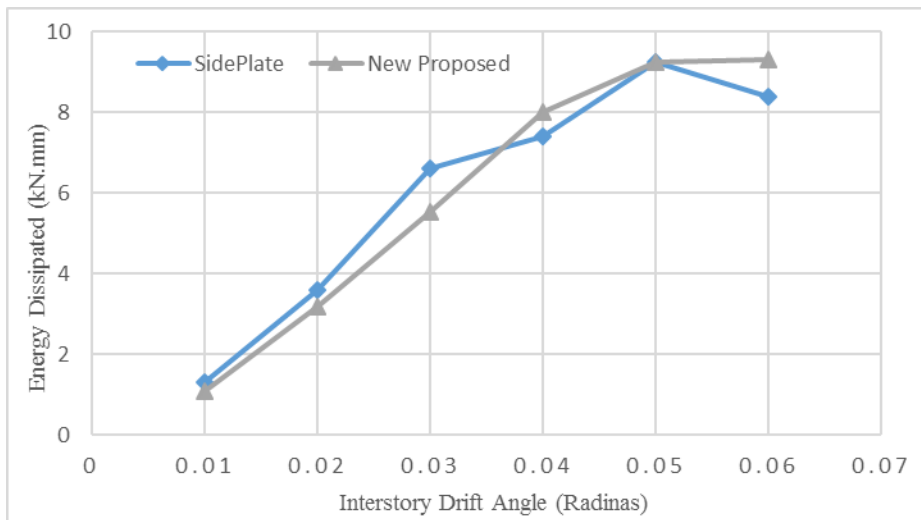

Figure 18: Energy dissipated for two connections.

5 SUMMARY OF FINDINGS AND CONCLUDING REMARKS

The seismic and progressive collapse performance of two different steel moment connections namely the SidePlate and new proposed moment connection was evaluated in this study. The fundamental acceptance criteria for seismic and progressive collapse evaluation used in this study include the interstory drift angle and flexural strength conforming to 2010 AISC Seismic Provisions[1] along

with plastic rotation angle conforming to UFC 4-023-03[23] guideline respectively. Based on the results of the experimental and numerical analyses, the following conclusions have been drawn:

I. Both the SidePlate and the proposed connection were capable of achieving adequate rotational capacity and developing the full inelastic capacity of the connecting beam.

II. Both the SidePlate and the proposed connection attained highe load and rotational capacities in progressive collapse test reaching around 3 times the external energy at first yielding.

III. According to the seismic performance test, one complete cycle of interstory drift angle of 0.06 rad was satisfied for both the SidePlate and new proposed connection which is an indication of the effectiveness of these two types of connections. Hence, application of these two types of connections in steel framed multi-story buildings is more effective against terrorist attacks and consequently, progressive collapse phenomenon.

IV. The maximum moment developed at beams was almost 1.20 times bigger than the actual beam plastic moment and also, the strain hardening value of 1.50 calculated according to FEMA 350 was exceeded in experimental tests.

V. The SidePlate and the new proposed connection system could reduce lateral steel tonnage due to connection stiffness that result in 100% rigid panel zone.

VI. The progressive collapse evaluation reveal that tensile capacities of beam–column joint after undergoing large rotations controlled the failure mode and the formation of catenary action. This implies that engineers should adopt high tensile resistances of beam–column joints after undergoing large rotations rather than pure tying resistance. If large rotation is not considered in the design stage, the joints with poor rotation capacities would fail to achieve the design tying resistances.

References

Agency, F. E. M. (2000). Recommended Seismic Evaluation and Upgrade Criteria for Existing Welded Steel Moment-Frame Buildings "FEMA 351". U. D. o. H. Security. United States of America.

Agency, F. E. M. (2000). Recommended Seismic Design Criteria for New Steel Moment-Frame Buildings "FEMA 350". U. D. o. H. Security. United States of America.

Beland, T., et al. (2014). Experimental Behavior of Bolted Angles and Beam-Column Connections. Structures Congress 2014, ASCE.

Chou, C. C., et al. (2010). "Seismic rehabilitation performance of steel side plate moment connections." Earthquake Engineering & Structural Dynamics 39(1): 23-44.

Construction, A. I. o. S. (2010). Prequalified Connections for Special and Intermediate Steel Moment Frames for Seismic Applications, AISC Connection Prequalification Review Panel.

Department of Defense (2010). Design of Buildings to Resist Progressive Collapse, UFC 4-023-03.

Han, S. W., et al. (2014). "Cyclic Performance of Welded Unreinforced Flange-Welded Web Moment Connections." Earthquake Spectra 30(4): 1663-1681.

Hedayat, A. A., et al. (2009). "Post-Northridge connection with modified beam end configuration to enhance strength and ductility." Journal of Constructional Steel Research 65(7): 1413-1430.

IBC, I. (2006). "International building code." International Code Council, Inc.(formerly BOCA, ICBO and SBCCI) 4051: 60478-65795.

Jalali, S., et al. (2012). "Probabilistic seismic demand assessment of steel moment frames with side-plate connections." Scientia Iranica 19(1): 27-40.

Jones, S. L., et al. (2002). "Experimental evaluation of cyclically loaded reduced beam section moment connections." Journal of Structural Engineering 128(4): 441-451.

Khandelwal, K., et al. (2011). "Pushdown resistance as a measure of robustness in progressive collapse analysis." Engineering Structures 33(9): 2653-2661.

Khandelwal, K., et al. (2009). "Progressive collapse analysis of seismically designed steel braced frames." Journal of Constructional Steel Research 65(3): 699-708.

Kim, J., et al. (2011). "Sensitivity analysis of steel buildings subjected to column loss." Engineering Structures 33(2): 421-432.

Kim, T., et al. (2002). "Experimental evaluation of plate-reinforced steel moment-resisting connections." Journal of Structural Engineering 128(4): 483-491.

Liu, J. (2010). "Preventing progressive collapse through strengthening beam-to-column connection, Part 1: Theoretical analysis." Journal of Constructional Steel Research 66(2): 229-237.

Olmati, P., et al. (2013). "Numerical analyses for the structural assessment of steel buildings under explosions." Structural Engineering and Mechanics 45(6): 803-819.

Ricles, J. M., et al. (2002). "Inelastic cyclic testing of welded unreinforced moment connections." Journal of Structural Engineering 128(4): 429-440.

Sabuwala, T., et al. (2005). "Finite element analysis of steel beam to column connections subjected to blast loads." International Journal of Impact Engineering 31(7): 861-876.

Saffari, H., et al. (2013). "Post-Northridge connections with slit dampers to enhance strength and ductility." Journal of Constructional Steel Research 80: 138-152.

Sofias, C., et al. (2014). "Experimental and FEM analysis of reduced beam section moment endplate connections under cyclic loading." Engineering Structures 59: 320-329.

Sun, R., et al. (2012). "Progressive collapse analysis of steel structures under fire conditions." Engineering Structures 34: 400-413.

The U.S. General Services Administration (2003). Progressive Collapse Design Guidelines Applied to Concrete Moment-Resisting Frame Buildings. Washington (DC).

Yang, B., et al. (2013). "Experimental tests of different types of bolted steel beam–column joints under a central-column-removal scenario." Engineering Structures 54: 112-130.